Memorias del XX Congreso Latinoamericano de Control Automático (CLCA 2025)
13-17 de Octubre, 2025. Cancún, Quintana Roo, México

Consensus Based Rendezvous for a pair of UAVs

Anaya Álvarez J. R. * **Martínez Clark R.** **
Chavez Guzmán C. *** **Flores Resendiz J. F.** ****
Avilés Velázquez J. D. †

Engeneering, Administrative and Social Sciences Faculty, Autonomous University of Baja California - Tecate BC

* *e-mail: ramon.anaya@uabc.edu.mx*
** *e-mail: rigoberto.martinez@uabc.edu.mx*
*** *e-mail: cchavez@uabc.edu.mx*
**** *e-mail: francisco.flores32@uabc.edu.mx*
† *e-mail: david.aviles@uabc.edu.mx*

Abstract:
This paper proposes a consensus-based protocol to achieve rendezvous between a pair of Unmanned Aerial Vehicles (UAVs), each controlled using a state-feedback linearization approach for trajectory tracking. Within this study, rendezvous is defined as the simultaneous arrival of the UAVs at a predetermined location. To accomplish this objective, the proposed protocol modulates the linear velocity of the UAVs—either amplifying or attenuating it—based solely on each aircraft's relative distance to the target position. Numerical simulations conducted using MATLAB/Simulink are presented to assess the feasibility of the proposed approach.

Keywords: Consensus, Rendezvous, UAV

1. INTRODUCTION

The study of UAVs (Unmanned Aerial Vehicles) has gained significant relevance in recent years across various sectors—including the research, industrial, civil, surveillance, and military communities—due to the wide range of applications for these devices.Such applications range from controlled laboratory research to surveillance, search and rescue missions, topographic analysis, agricultural irrigation, livestock monitoring, and numerous other fields. It is essential to understand the physical model that describes a UAV. The literature review in Reyes and Cid (2019) provide valuable insights into the physical effects involved in these systems and present a mathematical model that enables the analysis of various control strategies for successful vertical take-off, flight stability, and trajectory definition for these devices.

Building upon the control strategy design tools found in the literature Khalil (2015), simulation results of various methods are studied to identify the most effective solution to the aforementioned challenges. In Bouabdallah and Siegwart (2007), control techniques for nonlinear systems applied to UAVs are analyzed, including the design of a flight-stable controller.

The rendezvous problem encompasses different objectives. Sometimes, it is considered as a trajectory optimization problem Guffanti et al. (2024), or it involves the allocation of the rendezvous point. Do et al. (2025) and such in this case, simultaneous arrival to a predefined target. Achieving rendezvous in a group of UAVs will allow for the optimization of aircraft energy consumption, in addition to being useful in missions where the element of surprise is crucial, such as in surveillance. On the other hand, with simultaneous arrival, the group of robots can prepare for the emergence of complex collective behaviors such as cooperative transportation or foraging.

Several control strategies are found in the literature to address this problem. For example, Yan et al. (2024) employed a genetic algorithm for task allocation in a multi-UAV scenario, where simultaneous arrival and resource requirement constraints were considered during path planning generation. Conversely, Feng et al. (2024) considered a reinforcement learning strategy to address time constraints. Drawing from the approach proposed by Martínez-Clark et al. (2018), a consensus-based simultaneous arrival algorithm is presented. In this paper, a variable gain is defined that amplifies and atenuates the velocity of the UAVs in order to reach consensus in the distance to the rendezvous zone. After reaching consensus, the UAVs are driven to the rendezvous zone using a regulation controller.

The remainder of this document is structured as follows: Section 2 presents the design of a state-feedback linearization trajectory tracking controller for a UAV. Section 3 describes the consensus-based algorithm for the emergence of simultaneous arrival. Section 4 presents the results obtained through numerical simulations to validate the proposed control strategy, and finally, Section 5 outlines the conclusions drawn, as well as directions for future work.

https://doi.org/10.58571/CNCA.AMCA.2025.068

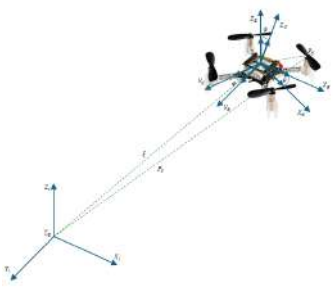

Fig. 1. Quadcopter model

2. UAV FEEDBACK LINEARIZATION

For this work, the quadcopter model (see Fig. 1) will be given by Bouabdallah and Siegwart (2007), given as follows:

$$X = \begin{bmatrix} \phi \\ \dot{\phi} \\ \theta \\ \dot{\theta} \\ \psi \\ \dot{\psi} \\ Z \\ \dot{Z} \\ X \\ \dot{X} \\ Y \\ \dot{Y} \end{bmatrix} = \begin{bmatrix} X_1 \\ X_2 \\ X_3 \\ X_4 \\ X_5 \\ X_6 \\ X_7 \\ X_8 \\ X_9 \\ X_{10} \\ X_{11} \\ X_{12} \end{bmatrix} \tag{1}$$

$$\dot{X} = \begin{bmatrix} X_2 \\ a_1 X_4 X_6 - a_2 X_4 \Omega_r + b_1 U_2 \\ X_4 \\ a_3 X_2 X_6 + a_4 X_2 \Omega_r + b_2 U_3 \\ X_6 \\ a_5 X_2 X_4 + b_3 U_4 \\ X_8 \\ g - (\cos X_1 \cos X_3) \left(\frac{1}{m}\right) U_1 \\ X_1 0 \\ U_x \left(\frac{1}{m}\right) U_1 \\ X_{11} \\ U_y \left(\frac{1}{m}\right) U_1 \end{bmatrix} \tag{2}$$

where

$$\begin{aligned} a_1 &= \frac{I_y - I_z}{I_x} \quad b_1 = \frac{l}{I_x} \\ a_2 &= \frac{J_r}{I_x} \quad\quad b_2 = \frac{l}{I_y} \\ a_3 &= \frac{I_z - I_x}{I_y} \quad b_3 = \frac{1}{I_z} \\ a_4 &= \frac{J_r}{I_y} \\ a_5 &= \frac{I_x - I_y}{I_z} \end{aligned} \tag{3}$$

$$\begin{aligned} U_x &= \cos X_1 \sin X_3 \cos X_5 + \sin X_1 \sin X_5 \\ U_y &= \sin X_1 \sin X_3 \cos X_5 - \cos X_1 \sin X_5 \end{aligned} \tag{4}$$

from (2), it is noticeable that the angular displacement is independent of the orthogonal (translational) components. On the other hand, the orthogonal components depend on the angular components in order to perform a translation in space. In this sense, system (2) has a cascade structure, with translational and attitude subsystems. This structure is depicted in Fig. 2.

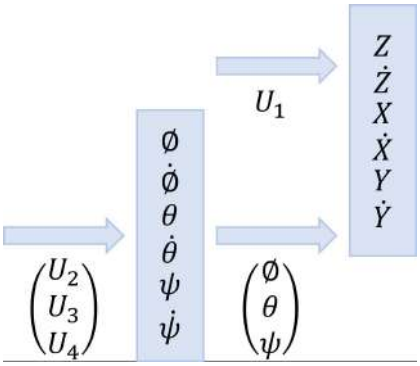

Fig. 2. From left to right, attitude and translation subsystems

The attitude subsystem is in the form of a third-order system which may derive in computational burden. Physically, this subsystem is prone to perturbations due to the harsh environment of the UAV. Thus, a second-order cascade system is proposed to reduce the complexity of signal processing. Taking the first states of (1) which correspond to ϕ and its derivative, the feedback linearization control Khalil (2015) is given as

$$\begin{aligned} \dot{X}_1 &= X_2 \\ \dot{X}_2 &= a_1 X_4 X_6 - a_2 X_4 \Omega_r + b_1 U_2 \end{aligned} \tag{5}$$

defining the error as:

$$e_1 = X_1 - r_2 \;\; e_2 = X_2 - \dot{r}_2 \tag{6}$$

Solving (6) yields

$$X_1 = e_1 + r_2 \;\; X_2 = e_2 + \dot{r}_2 \tag{7}$$

The first change of variables results from taking e_1 from (6) and taking its time derivative

$$\dot{e}_1 = \dot{X}_1 - \dot{r}_2 \tag{8}$$

from (5) and (7) it is given that

$$\dot{X}_1 = X_2 = e_2 + \dot{r}_2$$

solving (8) yields

$$\begin{aligned} \dot{e}_1 &= e_2 + \dot{r}_2 - \dot{r}_2 \\ \dot{e}_1 &= e_2 \end{aligned} \tag{9}$$

The same procedure is applied to e_2, yielding

 https://doi.org/10.58571/CNCA.AMCA.2025.068

$$\dot{e}_2 = \dot{X}_2 - \ddot{r}_2 \tag{10}$$

From (5) solving for $\dot{X}_2$

$$\dot{e}_2 = a_1 X_4 X_6 - a_2 X_4 \Omega_r + b_1 U_2 - \ddot{r}_2 \tag{11}$$

Next C is defined as

$$C = a_1 X_4 X_6 - a_2 X_4 \Omega_r - \ddot{r}_2 \tag{12}$$

Substituting (12) into (11)

$$\dot{e}_2 = C + b_1 U_2 \tag{13}$$

After the variable change, the system is described by (9) y (13)

$$\dot{e}_\phi = \begin{bmatrix} e_2 \\ C + b_1 U_2 \end{bmatrix} \tag{14}$$

where the field vector is defined by

$$f_{(e)} = \begin{bmatrix} e_2 \\ C \end{bmatrix}; g_{(e)} = \begin{bmatrix} 0 \\ b_1 \end{bmatrix}; h_{(e)} = e_1 + r_2$$

and

$$Y = h_{(e)}$$

given that

$$Y = e_1 + r_2 \tag{15}$$

the time derivative of Y is

$$\dot{Y} = \frac{\partial_h}{\partial_e}\left[f(e) + g(e)U\right] \stackrel{\text{def}}{=} L_f h(e) + L_g h(e) U \tag{16}$$

from the Lie derivative of h with respect to f it is obtained

$$L_f h(e) = \frac{\partial_h(e)}{\partial_e} f(e) = [1\ 0] \begin{bmatrix} e_2 \\ C \end{bmatrix}$$
$$L_f h(e) = e_2$$

that represents the first part of (16). The second part is obtained from the Lie derivative of h with respect to g, as follows

$$L_g h(e) = \frac{\partial_h(e)}{\partial_e} g(e) = [1\ 0] \begin{bmatrix} 0 \\ b_1 \end{bmatrix}$$
$$L_g h(e) = 0$$

substituting in (16)

$$\dot{Y} = e_2$$

It can be observed that $\dot{Y}$ is independent of U. Therefore, $\ddot{Y}$ is obtained from $h(e) = \dot{Y} = L_f h(e) = e_2$, calculating the second Lie derivative of h with respect to f as

$$L_f^2 h(e) = \frac{\partial_h(e)}{\partial_e} f(e) = [0\ 1] \begin{bmatrix} e_2 \\ C \end{bmatrix}$$
$$L_f^2 h(e) = C \tag{17}$$

and the Lie's derivative of h with respect to g, employing the notation $L_f L_g h(e)$ for convenience

$$L_f L_g h(e) = \frac{\partial_h(e)}{\partial_e} g(e) = [0\ 1] \begin{bmatrix} 0 \\ b_1 \end{bmatrix}$$

$$L_f L_g h(e) = b_1 \tag{18}$$

substituting (17) and (18) into (16) yields

$$\ddot{Y} = C + b_1 U_2 \tag{19}$$

in which the input U_2 can be observed.Through the input-output mapping, which is formed by a pair of integrators, the state-feedback controller is given as

$$U_2 = \frac{1}{L_f L_g h(e)} \left(-L_f^2 h(e) + v\right) \tag{20}$$

substituting (17) and (18) into (20)

$$U_2 = \frac{1}{b_1}\left(-C + v_2\right) \tag{21}$$

and eq. (12) into (21)

$$U_2 = \frac{1}{b_1}\left[-\left(a_1 X_4 X_6 - a_2 X_4 \Omega_r - \ddot{r}_2\right) + v_2\right]$$
$$U_2 = \frac{1}{b_1}\left(-a_1 X_4 X_6 + a_2 X_4 \Omega_r + \ddot{r}_2 + v_2\right) \tag{22}$$

the proposed control law

$$v_2 = -K_{21} * e_1 - K_{22} * e_2 \tag{23}$$

where the gains are

$$K_{21} = d_{21} * d_{22}$$
$$K_{22} = d_{22} + d_{22} \tag{24}$$

substituting (23) into (22) turns in the new control input for the state-feedback controller.

$$U_2 = \frac{1}{b_1}\left(-a_1 X_4 X_6 + a_2 X_4 \Omega_r + \ddot{r}_2 - K_{21} * e_1 - K_{22} * e_2\right) \tag{25}$$

Analogously, the procedure is employed for the remainder of the attitude subsystem, yielding the following control inputs

$$U_3 = \frac{1}{b_2}\left(-a_3 X_2 X_6 - a_4 X_2 \Omega_r + \ddot{r}_3 - K_{31} * e_3 - K_{32} * e_4\right) \tag{26}$$

$$U_4 = \frac{1}{b_3}\left(-a_5 X_2 X_4 + \ddot{r}_4 - K_{41} * e_5 - K_{42} * e_6\right) \tag{27}$$

Given the relationship of the angles ϕ and θ of the attitude subsystem with the orthogonal movements X and Y, the translation subsystem requires consideration of the angular displacement. Whith that in mind, the translational controller for the $X - Y$ plane outputs the references ϕ_d and θ_d Bouabdallah and Siegwart (2007). Considering the small angle approximation the rotational matrix

 https://doi.org/10.58571/CNCA.AMCA.2025.068

$$R = \begin{bmatrix} 1 & -\psi & \theta \\ \psi & 1 & -\phi \\ -\theta & \phi & 1 \end{bmatrix} \tag{28}$$

from eq. (2) and (28), simplifying the plane displacement dynamics yields

$$\begin{bmatrix} m\ddot{X} \\ m\ddot{Y} \end{bmatrix} = \begin{bmatrix} -\theta U_1 \\ \phi U_1 \end{bmatrix} \tag{29}$$

Given these considerations, the state-feedback controller for the translation subsystem is

$$U_1 = \frac{m}{\cos X_1 \cos X_3} \left(-g + \ddot{r}_1 - K_{11} * e_7 - K_{12} * e_8\right) \tag{30}$$

$$U_x = \frac{m}{U_1} \left(\ddot{r}_x - K_{x1} * e_9 - K_{x2} * e_{10}\right) \tag{31}$$

$$U_y = \frac{m}{U_1} \left(\ddot{r}_y - K_{y1} * e_1 1 - K_{y2} * e_{12}\right) \tag{32}$$

3. SIMULTANEOUS ARRIVAL RENDEZVOUS

Consider a pair of double integrator systems representing the distance towards a goal position as follows

$$\begin{aligned} \dot{\rho}_i &= v_i \\ \dot{v}_i &= u_i \;\; i = 1, 2 \end{aligned} \tag{33}$$

Where u is the control input and $\rho \in \Re^2$. One approach proposed in the literature is to represent the translation of system (33) as a unicycle wheeled mobile robot in polar coordinates Siegwart and Nourbakhsh (2004); Aicardi et al. (1995), by applying the following change of coordinates De Luca et al. (2001):

$$\begin{aligned} \rho &= \sqrt{x^2 + y^2}, \\ \gamma &= \text{ATAN2}(y, x) - \theta + \pi, \\ \delta &= \gamma + \theta, \end{aligned} \tag{34}$$

where ρ denotes the radial distance from the robot's position (x_r, y_r) to its desired goal position (x_g, y_g), γ represents the orientation error angle, measured from the robot's main axis to the pointing vector from (x, y) to (x_g, y_g) and, δ corresponds to the orientation with respect to the desired position frame (see Fig. 3). In polar coordinates, the kinematic model of the unicycle WMR can be represented as

$$\begin{aligned} \dot{\rho} &= -v \cos\gamma \\ \dot{\gamma} &= v \frac{\sin\gamma}{\rho} - \omega \\ \dot{\delta} &= v \frac{\sin\gamma}{\rho} \end{aligned} \tag{35}$$

Without loss of generality, the control objective can be addressed as the asymptotic regulation of the system (35) to the origin $(\rho = 0, \gamma = 0, \delta = 0)$, applying the following theorem

Theorem 1. (Aicardi et al. (1995)). Consider the kinematic model of a unicycle type WMR in polar coordinates (35), as well as the next control law

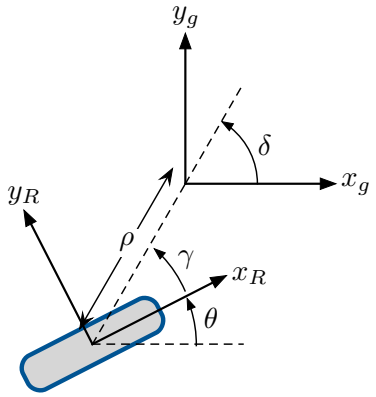

Fig. 3. Representation of the unicycle type WMR in polar coordinates.

$$\begin{aligned} v &= k_1 \rho \cos\gamma \\ \omega &= k_2 \gamma + k_1 \frac{\sin\gamma \cos\gamma}{\gamma} (\gamma + k_3 \delta) \end{aligned} \tag{36}$$

with $k_1, k_2, k_3 \in \Re^+$. Therefore, the closed loop system (35)-(36) asymptotically converges to the state $(\rho(t), \gamma(t), \delta(t)) = (0, 0, 0)$ as $t \to \infty$, manoeuvring like the natural driving of a motor vehicle by a person.

The assumption of natural driving maneuvering of Theorem 1, refers to the motion of the robot with positive linear velocity towards the desired position. In this case, $\gamma \to 0$ in order to drive the robot along the vector $\boldsymbol{\rho}$.

In this work, rendezvous task is considered as the simultaneous arrival of a pair of WMR to a previously known position in a obstacle-free workspace. To achieve this goal, the robots employ a consensus protocol based on their distances to the goal. This approach assumes that if both robots use the same regulation controller to reach the rendezvous point, they will arrive simultaneously, provided they start at the same distance from this landmark. The reduction of the distance error for a pair of wheeled mobile robots represented in polar coordinates is achieved through the rendezvous gain described in the following theorem

Theorem 2. (Distance consensus protocol). A pair of WMR represented in polar coordinates will simultaneously arrive (by means of distance consensus) to the rendezvous point, if control (36) multiplied by the next rendezvous gain is employed

$$K_{r_i} = 1 + \left(\frac{\rho_i - \rho_j}{\max\left(\rho_i, \rho_j\right)} \right) \tag{37}$$

Accordingly, the control inputs for robot i are as follows:

$$\begin{aligned} v &= K_{r_i} k_1 \rho \cos\gamma \\ \omega &= K_{r_i} (k_2 \gamma + k_1 \frac{\sin\gamma \cos\gamma}{\gamma} (\gamma + k_3 \delta)) \end{aligned} \tag{38}$$

Proof. Consider the distance to rendezvous point error of robots i and j as $e_\rho = \rho_i - \rho_j$. The dynamics of the distance error are given by

$$\begin{aligned} \dot{e}_\rho &= \dot{\rho}_i - \dot{\rho}_j \\ \dot{e}_\rho &= -v_i \cos\gamma_i + v_j \cos\gamma_j \end{aligned} \tag{39}$$

replacing (36) and (37) into (39) yields

 https://doi.org/10.58571/CNCA.AMCA.2025.068

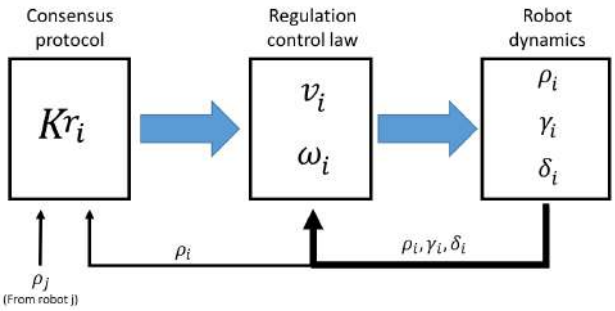

Fig. 4. Relationship between robot dynamics, regulation control law and the proposed consensus protocol.

$$-\left(1+\frac{e\rho}{max(\rho_i,\rho_j)}\right)\rho_i\cos^2\gamma_i+\left(1-\frac{e\rho}{max(\rho_i,\rho_j)}\right)\rho_j\cos^2\gamma_j \tag{40}$$

Considering that in the regulation controller (36) the orientation error diminishes in order to drive the robot in a straight line to the desired landmark, this is $\gamma \to 0$. This entails that $\cos^2\gamma \to 1$. Therefore, the distance error dynamics are given by

$$\dot{e}_\rho = -e_\rho(1+\frac{\rho_i+\rho_j}{max(\rho_i,\rho_j)}) \tag{41}$$

This demonstrates that the origin of the e_ρ dynamics is exponentially stable; consequently, the robots will equalize their distances to the rendezvous point.

Multiplying the consensus protocol (37) by the regulation control law (36) as shown in (38), amplifies the control inputs of the robot with a greater distance to the rendezvous point, up to a maximum factor of two. Conversely, the control inputs of the robot closest to the rendezvous point will be attenuated, with a lower bound of zero, corresponding to the robot being exactly at the rendezvous point. The relationship between the consensus protocol and the regulation control law is depicted in Fig. 4.

4. RESULTS

To achieve simultaneous arrival rendezvous for a pair of UAVs, the proposed scheme employs the rendezvous protocol for the double integrator agents as an input to the translational state-feedback controller (30) - (32), thereby driving both UAVs to the rendezvous point.

Numerical simulations were performed using MATLAB/Simulir R2018a on a laptop with the following characteristics:

- Operating system: Windows 10 64 bits
- Processor: AMD Ryzen 5 3500U with Radeon Vega Mobile Gfx 2.10 GHz
- RAM: 12 GB

Fig. 5 shows the block diagram of the system. Each block represents one UAV with the state-feedback controller and the small block on the left is the rendezvous protocol

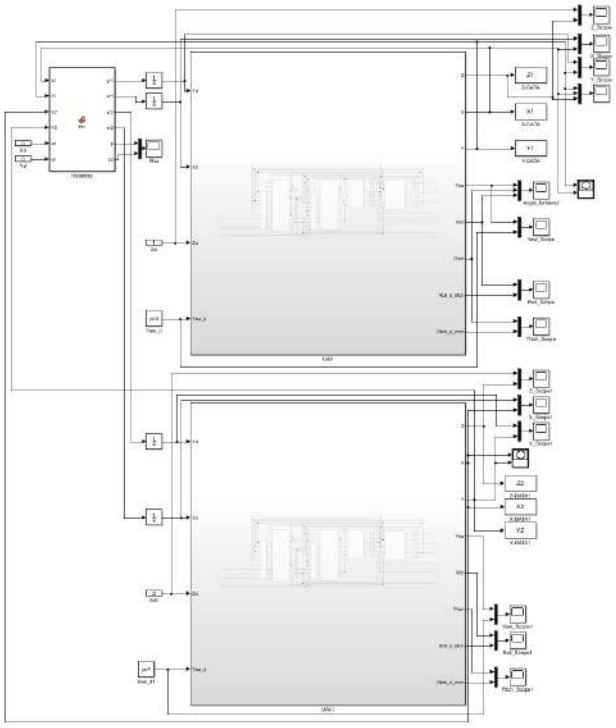

Fig. 5. Simulink Simultaneous arrival

The initial positions of the UAVs were arbitrarily selected as

- UAV 1 (4,-20,0.1)[m]
- UAV 2 (8,20,3)[m]

The rendezvous point is defined as $X = 0$, $Y = 0$. To avoid collisions, UAV 1 is driven to Z=1 while UAV2 is driven to z=1.5. Fig. 6 shows the trajectories of the UAVS towards the rendezvous points. Fig. 7 depicts the distance ρ of both UAV. This Figure demonstrates that both UAVs achieve consensus on their distance to the rendezvous area and arrive simultaneously.

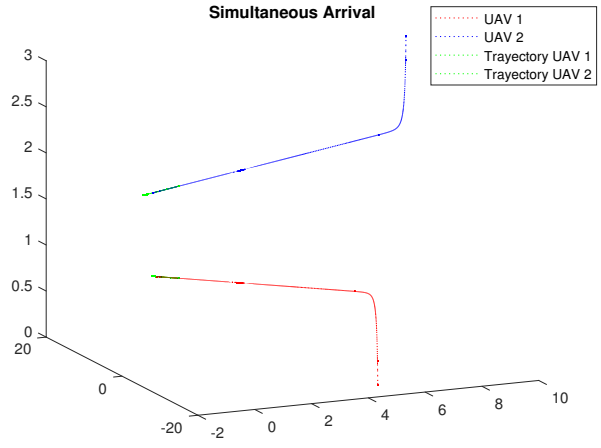

Fig. 6. UAVs trajectories in the workspace

On the other hand, Fig. 7 shows the distance ρ of each UAV across time, where the simultaneous arrival is evidentiated.

https://doi.org/10.58571/CNCA.AMCA.2025.068

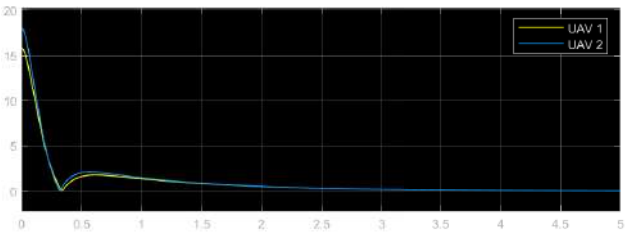

Fig. 7. UAV distance to rendezvous zone Comparison

5. CONCLUSIONS

The consensus algorithm for simultaneous arrival is based on the analysis of translation in polar coordinates of an agent, such as a wheeled mobile robot. When used as input for state-feedback trajectory tracking control of a UAV, the results obtained with a different type of vehicle (e.g., a WMR) can be extrapolated. The main advantage of the communication protocol is that only the distance of each robot to the rendezvous point is shared. This prevents the communication channel from becoming saturated, thereby enhancing feasibility for implementation on physical robotic platforms. As future work, the aim is to analyze other trajectory tracking control strategies for UAVs that are compatible with this consensus algorithm, and to pursue experimental results using commercial UAVs.

REFERENCES

Aicardi, M., Casalino, G., Bicchi, A., and Balestrino, A. (1995). Closed loop steering of unicycle like vehicles via Lyapunov techniques. *IEEE Robotics & Automation Magazine*, 2(1), 27–35.

Bouabdallah, S. and Siegwart, R. (2007). Full control of a quadrotor. In *2007 IEEE/RSJ international conference on intelligent robots and systems*, 153–158. Ieee.

De Luca, A., Oriolo, G., and Vendittelli, M. (2001). Control of Wheeled Mobile Robots: An Experimental Overview. In S. Nicosia, B. Siciliano, A. Bicchi, and P. Valigi (eds.), *Articulated and Mobile Robotics for Services and Technologies*, 181–226. Springer Berlin Heidelberg.

Do, H., Jang, J., and Kim, J. (2025). Heterogeneous multi-robot system mission planning with cooperative replenishment through data-driven rendezvous point selection. *Intelligent Service Robotics*, 18(1), 61–73.

Feng, J., Fan, L., Hu, J., Xu, Z., and Han, J. (2024). Multi-target penetration path planning for uav swarms based on time synchronization constraints. In *International Conference on Guidance, Navigation and Control*, 71–80. Springer.

Guffanti, T., Gammelli, D., D'Amico, S., and Pavone, M. (2024). Transformers for trajectory optimization with application to spacecraft rendezvous. In *2024 IEEE Aerospace Conference*, 1–13. IEEE.

Khalil, H.K. (2015). Nonlinear control.

Martínez-Clark, R., Cruz-Hernández, C., Pliego-Jimenez, J., and Arellano-Delgado, A. (2018). Control algorithms for the emergence of self-organized behaviours in swarms of differential-traction wheeled mobile robots. *International Journal of Advanced Robotic Systems*, 15(6), 1729881418806435.

Reyes, F. and Cid, J. (2019). Drones. cinemática, dinámica y control de cuadricópteros.

Siegwart, R. and Nourbakhsh, I.R. (2004). *Introduction to Autonomous Mobile Robots*, volume 23. MIT press.

Yan, F., Chu, J., Hu, J., and Zhu, X. (2024). Cooperative task allocation with simultaneous arrival and resource constraint for multi-uav using a genetic algorithm. *Expert Systems with Applications*, 245, 123023.

 https://doi.org/10.58571/CNCA.AMCA.2025.068